

ORIGINAL ARTICLE

A role for FOXO1 in BCR–ABL1-independent tyrosine kinase inhibitor resistance in chronic myeloid leukemia

M Wagle¹, AM Eiring², M Wongchenko¹, S Lu¹, Y Guan¹, Y Wang¹, M Lackner¹, L Amler¹, G Hampton¹, MW Deininger^{2,3}, T O'Hare^{2,3,4} and Y Yan^{1,4}

Chronic myeloid leukemia (CML) patients who relapse on imatinib due to acquired ABL1 kinase domain mutations are successfully treated with second-generation ABL1-tyrosine kinase inhibitors (ABL-TKIs) such as dasatinib, nilotinib or ponatinib. However, ~40% of relapsed patients have uncharacterized BCR–ABL1 kinase-independent mechanisms of resistance. To identify these mechanisms of resistance and potential treatment options, we generated ABL-TKI-resistant K562 cells through prolonged sequential exposure to imatinib and dasatinib. Dual-resistant K562 cells lacked *BCR–ABL1* kinase domain mutations, but acquired other genomic aberrations that were characterized by next-generation sequencing and copy number analyses. Proteomics showed that dual-resistant cells had elevated levels of FOXO1, phospho-ERK and BCL-2, and that dasatinib no longer inhibited substrates of the PI3K/AKT pathway. In contrast to parental cells, resistant cells were sensitive to growth inhibition and apoptosis induced by the class I PI3K inhibitor, GDC-0941 (pictilisib), which also induced FOXO1 nuclear translocation. FOXO1 was elevated in a subset of primary specimens from relapsed CML patients lacking *BCR–ABL1* kinase domain mutations, and these samples were responsive to GDC-0941 treatment *ex vivo*. We conclude that elevated FOXO1 contributes to BCR–ABL1 kinase-independent resistance experienced by these CML patients and that PI3K inhibition coupled with BCR–ABL1 inhibition may represent a novel therapeutic approach.

Leukemia (2016) 30, 1493–1501; doi:10.1038/leu.2016.51

INTRODUCTION

Chronic myeloid leukemia (CML) is a hematopoietic disease in which the majority of patients express the chimeric BCR–ABL1 oncoprotein, product of the reciprocal t(9;22) (q34;q11) translocation, which generates a shortened chromosome 22 called the Philadelphia (Ph) chromosome.¹ Approximately 85% of patients diagnosed in chronic phase are effectively treated with the small-molecule ABL1-tyrosine kinase inhibitor (ABL-TKI), imatinib.² Other approved ABL-TKIs such as nilotinib, dasatinib and ponatinib were developed to clinically overcome imatinib resistance. However, residual Ph⁺ cells persist even in patients responding well to ABL-TKI therapy, indicating that these drugs do not eliminate the quiescent Ph⁺ stem cell population.¹ Therefore, to prevent disease progression, patients undergo prolonged treatment with sequential ABL-TKIs to control the growth of Ph⁺ progenitors.

Prolonged exposure to ABL-TKIs leads to acquired resistance in up to 40% of CML patients.¹ Mechanisms of acquired resistance include amplification of the *BCR–ABL1* gene and the acquisition of point or compound mutations in the *BCR–ABL1* kinase domain.^{3–5} Alternatively, activation of downstream signaling pathways such as PI3K, MAPK or JAK/STAT may lead to drug resistance in a BCR–ABL1 kinase-independent manner.^{6–10} Therefore, inhibitors targeting these pathways in combination with ABL-TKIs may represent alternative therapeutic approaches.

Downstream of the PI3K pathway are the FOXO transcription factors that can regulate differentiation, proliferation, tumor suppression and cell death. Phosphorylation of FOXOs by AKT

leads to cytoplasmic sequestration, ubiquitination and proteasomal degradation.^{11,12} A number of studies have shown the importance of FOXOs, especially FOXO3a, in maintenance of the hematopoietic system and drug resistance.^{13–16} Indeed, it was recently shown that BCR–ABL1 induces phosphorylation of FOXOs, leading to their cytoplasmic localization in primary CML CD34⁺ cells compared with normal progenitors, which is reversed when TKI-sensitive cells are treated with ABL-TKIs *ex vivo*.¹⁷

The aim of this study was to identify genetic and protein expression/phosphorylation changes associated with acquired BCR–ABL1 kinase-independent resistance. Using reverse-phase protein arrays, we identified elevated levels of FOXO1, phospho-ERK and BCL-2 in CML cell lines and patient samples with kinase-independent resistance. These cells had increased sensitivity to PI3K inhibition, but no change in sensitivity to MEK inhibition. Our data suggest that, for certain CML patients with BCR–ABL1 kinase-independent resistance, it may be beneficial to combine PI3K inhibitors with approved ABL-TKIs such as imatinib.

MATERIALS AND METHODS

Chemicals

Imatinib, dasatinib and ponatinib were obtained from Selleck Chemicals (Houston, TX, USA). GDC-0941 (pictilisib) and GDC-0973 (cobimetinib) were manufactured at Genentech (South San Francisco, CA, USA). All the chemicals were resuspended to 10 mM in dimethyl sulfoxide (DMSO). Clinically relevant exposures of these drugs are in the 300–1000 nM range.

¹Oncology Biomarker Development, Genentech, South San Francisco, CA, USA; ²Huntsman Cancer Institute, The University of Utah, Salt Lake City, UT, USA and ³Division of Hematology and Hematologic Malignancies, The University of Utah, Salt Lake City, UT, USA. Correspondence: Dr T O'Hare, Huntsman Cancer Institute, The University of Utah, 2000 Circle of Hope, Room 4264, Salt Lake City, UT 84112, USA or Dr Y Yan, Oncology Biomarker Development, Genentech, 1 DNA Way, South San Francisco, CA 94080, USA. E-mail: thomas.ohare@hci.utah.edu or yan.yibing@gene.com

⁴These authors contributed equally to this work

Received 15 September 2015; revised 29 January 2016; accepted 18 February 2016; accepted article preview online 8 March 2016; advance online publication, 5 April 2016

Cell lines

The K562 cell line (American Type Culture Collection: ATCC, Manassas, VA, USA) and the KCL-22 cell line (Deutsche Sammlung von Mikroorganismen und Zellkulturen GmbH: DSMZ, Braunschweig, Germany) were cultured in RPMI-1640 containing 10% FBS in 5% CO₂ at 37 °C. The dual-resistant K562 cells and clones were generated by exposing K562 cells to increasing concentrations of imatinib (0–10 μM) over a 6-month period. The resistant cells were then exposed to increasing concentrations of dasatinib (0–200 nM), resulting in dual resistance. Imatinib-resistant cells were maintained in 1 μM imatinib; dual-resistant cells and clones were maintained in high doses of dasatinib (50 nM) to avoid reversion to a non-resistant state. The dual-resistant KCL-22 cells were isolated through exposure of the parental cells to 10 μM imatinib over 10 days following a previously published protocol.¹⁸

Patient samples

CD34⁺-enriched (purity >90%; Miltenyi Biotech, San Diego, CA, USA) specimens from patients who had relapsed from imatinib, dasatinib and/or nilotinib (Supplementary Table S1) were provided by Drs Michael W Deininger and Thomas O'Hare at The University of Utah Huntsman Cancer Institute (Salt Lake City, UT, USA). All donors gave informed consent and all studies were approved by The University of Utah Institutional Review Board.

Cell viability assays and combination studies

Dual-resistant KCL-22 and K562 cells and clones were seeded at 5000 cells/well in 96-well plates. Cell viability was measured using CellTiter-Glo reagent as per the manufacturer's instructions and ATP measurements were read using an Envision reader (PerkinElmer, Waltham, MA, USA). Baseline day 0 cell viability was measured 24 h after cell seeding. The cells were treated in triplicate for 72 h with 0–10 μM concentrations of imatinib, dasatinib, GDC-0941 or GDC-0973 diluted in growth medium. For drug combination studies, the cells were seeded in quadruplicate plates and treated for 72 h with increasing doses of one drug (0–10 μM) in combination with increasing doses of the second drug (0–10 μM). An R script was used to generate heat maps showing percent growth inhibition at each treatment combination (R open-source software).

Immunoblots

Ten micrograms of total protein from each sample was resolved on a 4–12% Bis-Tris gel using MOPS buffer (Invitrogen, NY, USA). Following the transfer, blots were incubated with blocking buffer (LI-COR Biosciences, Lincoln, NE, USA) and stained overnight with primary antibodies (see Supplementary Table S2). The blots were stained with IR dye-conjugated secondary antibodies and imaged using a LI-COR Odyssey scanner.

Apoptosis assays

Dual-resistant and parental K562 cells were treated for 48 h with vehicle, 50 nM dasatinib or 300 nM GDC-0941 to assess early apoptosis. The cells were stained with FITC-conjugated Annexin V and propidium iodide followed by analysis using a FACS-calibur cytometer (Becton Dickinson, Franklin Lakes, NJ, USA).

Next-generation sequencing and copy number analyses

Genomic DNA from dual-resistant K562 and KCL-22 cells and clones was isolated and sequenced using the GAII Ultra-deep sequencing platform (Illumina, San Diego, CA, USA). The data were filtered using a 10% variant frequency cutoff. For copy number analysis, DNA from resistant cells and clones was run on the Oncoscan2 platform (Affymetrix, Santa Clara, CA, USA) and analyzed using Nexus Copy Number software (BioDiscovery, Hawthorne, CA, USA).

Proteomic analysis using reverse-phase protein arrays

Dual-resistant K562 and KCL-22 cells were treated for 1 h with DMSO, 50 nM dasatinib, 300 nM GDC-0941 or 300 nM GDC-0973 to capture phosphorylation changes, before lysis in a buffer containing tissue protein extraction reagent (T-PER, ThermoFisher Scientific, Waltham, MA, USA), 300 mM NaCl, and protease and phosphatase inhibitors (Sigma-Aldrich, St. Louis, MO, USA). Lysates of CD34⁺ cells from treatment-naive ($n=3$) and

ABL-TKI-treated patients with BCR-ABL1 kinase-dependent or kinase-independent resistance ($n=16$) were also prepared. Where indicated, some patient samples were treated *ex vivo* with 50 nM dasatinib for 4 h to assess pCRKL Y207. The samples were assessed by reverse-phase protein array (RPPA) analysis (Theranostics Health, Rockville, MD, USA) using 30 validated antibodies (Supplementary Table S2). Quadruplicate samples were printed onto nitrocellulose slides in four separate quadrants. Total protein was measured by sypro-stain, and the intensities of specific antibody signals were subtracted from secondary antibody signal and normalized to the total protein (to account for differences in protein content between samples). The data from each slide were normalized to the median of each quadrant to compensate for spatial effects. For more details on the RPPA data analysis, see the 'Statistics' section below.

FOXO1 immunofluorescence

Parental and dual-resistant K562 cells were treated with either DMSO, 100 nM dasatinib or 1 μM GDC-0941 for 1 h, fixed in 4% paraformaldehyde, blocked in 0.3% Triton/5% goat serum and stained with a FOXO1-specific antibody (Cell Signaling Technology, Danvers, MA, USA) or goat IgG overnight at 4 °C. After staining with an anti-goat Alexa-488-conjugated antibody and DAPI (Cell Signaling Technology) for 1 h at room temperature, the cells were analyzed on a Leica confocal microscope with ×40 objective and the images were captured using Leica application suite software (Leica Microsystems, Buffalo Grove, IL, USA).

Stable knockdown of FOXO1 using short hairpin RNA (shRNA)

Non-targeting, FOXO1, FOXO3 and GAPDH shRNA lentiviral particles (Supplementary Table S3, Dharmacon GE Lifesciences, Lafayette, CO, USA) were used to transduce 0.5×10^6 parental and dual-resistant K562 cells in the presence of 5 ng/ml polybrene in RPMI. Following puromycin selection, knockdown was confirmed by immunoblot analysis, and transduced cells were seeded into 96-well plates for treatment with 0–100 nM dasatinib or 0–1000 nM GDC-0941 for 72 h in triplicate for viability assay with CellTiter-Glo as described previously.

Colony assays and short-term viability assays

Methylcellulose colony assays were performed by plating 10^3 CML CD34⁺ patient samples in 0.9% MethoCult (H4230; StemCell Technologies, Vancouver, BC, Canada) in the presence or absence of the indicated inhibitors. All colony assays were performed in the presence of $1 \times$ CC100 (StemCell Technologies) and scored after 14–21 days in culture in a humid chamber.

Statistics

To ensure adequate statistical power, all data represent three independent experiments unless otherwise stated. Quadrant-median normalized RPPA data from the resistant cell lines and patient samples were log₂-transformed to assume a normal distribution and normalized to baseline control (parental K562 or KCL-22 cells or treatment-naive patient samples) before analysis using Partek Genomics Suite (Partek, St. Louis, MO, USA). Protein expression/phosphorylation in the dual-resistant cells or patient samples were contrasted to the expression of the same proteins in their respective controls using a one-way analysis of variance or parametric unpaired *t*-tests for data with equal variance in GraphPad Prism (GraphPad Software Inc., La Jolla, CA, USA). Significant differences in protein expression between cell types were considered as being >1.6-fold with a *P*-value < 0.05. For colony data with patient specimens, growth of the vehicle-treated control was set at 100% and a two-tailed Student's *t*-test for unequal variances was used.

RESULTS

Sensitivity of parental and resistant K562 and KCL-22 cell lines to multiple ABL-TKIs

The dual-resistant cell lines were generated by prolonged treatment of K562 cells with imatinib followed by dasatinib to mimic the treatment regimen that most patients receive in the clinic upon diagnosis and imatinib relapse. We first compared the sensitivity of imatinib- and dual-resistant cells to 0–10 μM imatinib, dasatinib and ponatinib to parental controls. Figure 1a shows the

response of each resistant cell line to 0.001–10 μM ABL-TKI as % growth, corrected to the day 0 growth rate and plotted relative to the DMSO control (set to 100%). With this method, the cell

growth rates after treatment are compared with those before treatment (that is, zero % growth represents cell stasis and negative % growth represents cell death). The raw data are shown

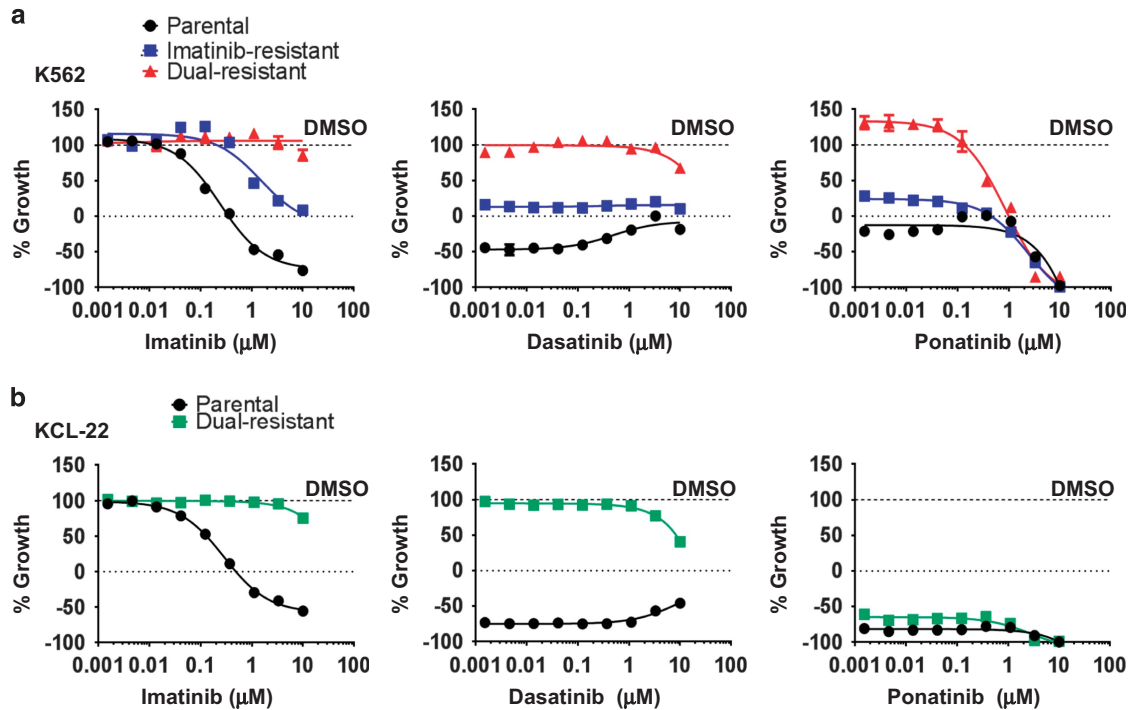


Figure 1. Imatinib and dual-resistant K562 cells are resistant to all three ABL-TKI therapies, whereas the KCL-22 cells are highly sensitive to ponatinib. (a) Sensitivity of the K562 parental, imatinib- and dual-resistant cell lines to 0–10 μM imatinib, dasatinib or ponatinib after treatment for 72 h as measured by CellTiter-Glo assays. (b) Sensitivity of the KCL-22 parental and resistant cells to 0–10 μM imatinib, dasatinib or ponatinib after treatment for 72 h as measured by CellTiter-Glo assays. The cell viability was measured and corrected relative to time zero (time of treatment). The data shows % control 0.001–10 μM ABL-TKI-treated cells relative to vehicle (DMSO)-treated cells, which is set to 100% growth (upper dotted line). The data represent the average of three independent experiments. The error bars represent standard deviation.

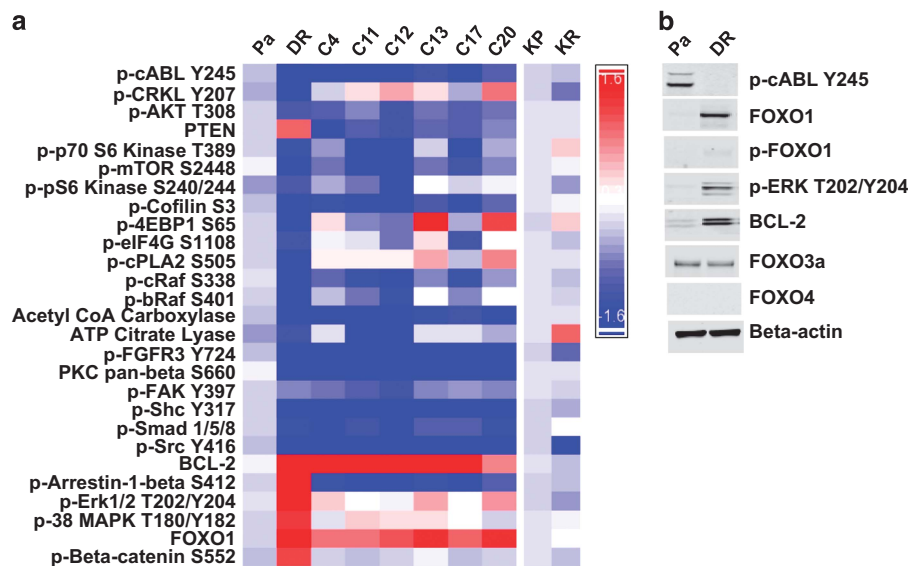


Figure 2. Reverse-phase protein arrays reveal elevated levels of p-ERK, BCL-2 and FOXO1 in TKI-resistant versus parental K562 cells. (a) The baseline proteomic signature of the parental K562 cells (Pa) is compared with the dual-resistant cells (DR) and resistant clones (C4–C20). The baseline proteomic signature of the parental KCL-22 cells (KP) compared with the resistant KCL-22 cells (KR) is also shown. The data are log₂-transformed and normalized to the respective parental cell line. Only the end points that show a > 1.6-fold difference between the resistant cells and their respective parental cells are shown. (b) Immunoblot analyses confirmed elevated levels of FOXO1, p-ERK T202/Y204 and BCL-2 expression, as well as decreased p-ABL Y245, in the dual-resistant cells compared with the parental cell line. FOXO3a, FOXO4 and beta-actin were analyzed as controls.

in Supplementary Figure S1. The parental K562 cell line was sensitive to imatinib (GI50: 0.3 μM), and highly sensitive to dasatinib and ponatinib treatment (GI50: < 0.001 μM ; Figure 1a). The imatinib-resistant cells were only resistant to imatinib, whereas the dual-resistant cells were resistant to doses of imatinib and dasatinib up to 10 μM , and even demonstrated some resistance to the ABL-TKI, ponatinib (GI50: 0.86 μM) (Figure 1a), which is efficacious against all the *BCR-ABL1* kinase domain mutations including T315I.¹⁹ In contrast, the resistant KCL-22 cells were highly sensitive to ponatinib despite being resistant to both imatinib and dasatinib (Figure 1b). Altogether, these data suggest that while the KCL-22 resistant cells likely harbor a *BCR-ABL1* kinase domain mutation,¹⁸ the dual-resistant K562 cells may have a BCR-ABL-independent mechanism of resistance. In support of this, the direct substrate of the BCR-ABL kinase, pCRKL, was inhibited in the dual-resistant K562 cells despite being resistant to dasatinib-mediated cell death (Supplementary Figure 2a).

Next-generation sequencing and copy number analysis of the resistant cell lines

We sequenced the parental and resistant cell lines with a panel of 86 oncogenes and tumor suppressor genes using the Illumina deep sequencing platform, GAll.²⁰ We also did copy number analysis using the Affymetrix Oncoscan2 MIP array. None of the K562-resistant cells and clones had acquired *BCR-ABL1* kinase domain mutations (Supplementary Table 4a). Furthermore, although the dual-resistant K562 cells and clones had acquired multiple new mutations and copy number alterations, there were no amplifications of *ABL1*, a known mechanism of ABL-TKI resistance (Supplementary Tables 4a–c). Mutations present in multiple clones included the chromatin remodeling gene, SMARCA4, and the tumor suppressor gene, NF-2. Somatic mutations in both of these proteins have been characterized in patient tumors.^{21,22} In contrast, the dual-resistant KCL-22 cells, which harbored a T315I kinase domain mutation (Supplementary Table 4a), acquired relatively few additional genetic changes. Despite the many genetic aberrations in the dual-resistant K562 cells due to clonal heterogeneity, no common signaling pathway was identified that could explain resistance. Therefore, we moved forward with a more functional proteomics approach.

Proteomic analysis of ABL-TKI-resistant cells and clones by RPPA

We assessed the baseline expression and phosphorylation changes in proteins between the parental (Pa) and dual-resistant cells and clones (C4–C20) by RPPA (Figure 2a). The proteins demonstrating a > 1.6-fold difference between the parental and dual-resistant cells or clones are shown as a heat map in Figure 2a. p-ABL1 Y245, pCRKL Y207, p-AKT T308 and downstream AKT substrates such as p-p70 S6 kinase T389, p-Cofilin S3 and p-mTOR S2448, had significantly lower baseline expression levels in the dual-resistant cells compared to the parental cells. Total BCL-2 and total FOXO1 were significantly elevated in all the dual-resistant cells and clones, whereas p-ERK Y202/T204 was elevated only in the dual-resistant cells and in clones 4, 13 and 20 compared with parental controls. These data are confirmed in Figure 2b in addition to data showing that levels of p-FOXO1 and other FOXO family members, including FOXO3a and FOXO4, were not significantly different between parental and dual-resistant K562 cell lines.

Very few proteins were differentially regulated in the resistant KCL-22 cells compared with the parental KCL-22 cells (Figure 2a). Altogether, these data show that dual-resistant K562 cells have distinct patterns of pathway activation not seen in kinase-mutated KCL-22 cells, involving effectors of the ERK and PI3K pathways.

Sensitivity of ABL-TKI-resistant K562 and KCL-22 cells to PI3K or MAPK inhibition

To confirm the involvement of these pathways in resistance, we tested the effects of the pan-PI3K inhibitor, GDC-0941 (0–10 μM) or the MEK inhibitor, GDC-0973 (0–10 nM), on the viability of parental and dual-resistant cells *in vitro* (Figure 3a). The dual-resistant K562 cells were 100-fold more sensitive to GDC-0941 (GI50 20 nM) than the parental cell line (GI50 2 μM). In contrast, sensitivity to GDC-0973 was similar between the lines (Figure 3a), despite the dual-resistant cells having higher levels of p-ERK (Figure 2). All dual-resistant cell clones were more sensitive to GDC-0941 (10–20-fold) and some even showed resistance to GDC-0973 (2–10-fold) compared to parental cells (Table 1). In contrast, the parental and resistant KCL-22 cells were insensitive to growth inhibition by either compound (Figure 3a and Table 1). Accordingly, GDC-0941 (Figure 3b) but not GDC-0973 (data not shown) induced early apoptosis in dual-resistant but not parental K562 cells. Thus, the PI3K pathway is suspected to be the predominant pathway involved in resistance.

Modulation of phosphoproteins by dasatinib and GDC-0941

Next, we assessed the effects of these inhibitors on phosphoproteins in the PI3K and MAPK pathways using RPPA. We treated the

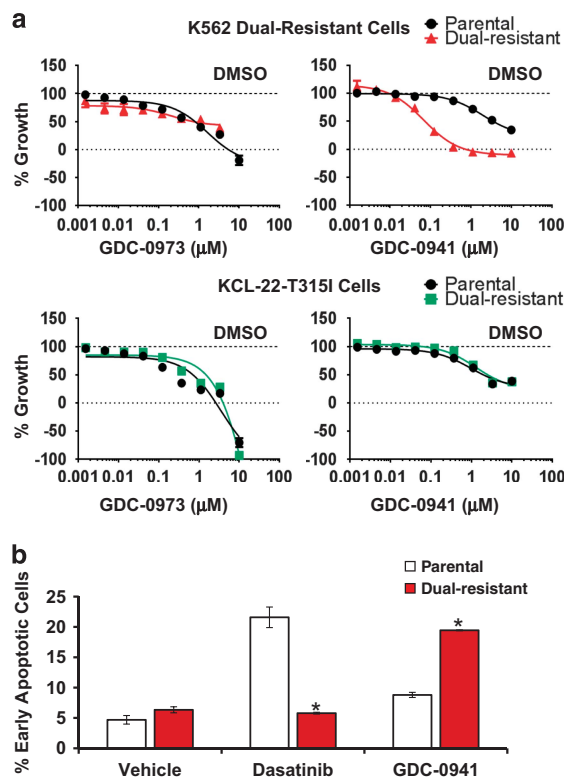


Figure 3. Dual-resistant cells and clones are sensitive to GDC-0941-mediated growth inhibition (a) Sensitivity of the dual-resistant K562 cells and resistant KCL-22 cells to 0–10 μM GDC-0941 or 0–10 μM GDC-0973 after 72 h treatment. The cells were treated for 72 h with the indicated drug and cell viability was measured and corrected relative to time zero (time of treatment). The data shows % control 0.001–10 μM TKI-treated cells relative to vehicle (DMSO)-treated cells, which is set to 100% (upper dotted line). The data represent the average of three independent experiments. The error bars represent standard deviation. (b) The percentage of cells undergoing early apoptosis induced by 50 nM dasatinib or 300 nM GDC-0941 in the dual-resistant and parental K562 cells 48 h after treatment using AnnexinV/PI FACS analysis. The error bars represent standard deviation. * $P < 0.05$.

cells with either vehicle, 100 nM dasatinib, 300 nM GDC-0941 or 300 nM GDC-0973. p-AKT T308, p-ERK T202/Y204 and the AKT substrates p-PRAS40 T246 and p-p70 S6 kinase T389, were all significantly inhibited by dasatinib in the parental K562 cell line (Figures 4, $P < 0.0001$). In contrast, dasatinib significantly increased p-ERK T202/Y204, p-PRAS40 T246 and p-p70 S6 T389 kinase in the dual-resistant line (Figure 4). In both the parental and dual-resistant cells, p-ERK T202/Y204 was inhibited by GDC-0973, despite having no effect on cell growth (Figure 3a). Furthermore, the AKT substrates p-PRAS40 T246 and p-p70 S6 kinase T389 were significantly inhibited by GDC-0941, as was p-AKT T308 ($P < 0.0001$). Neither the expression of FOXO1 nor BCL-2 was altered by dasatinib, GDC-0941 or GDC-0973 in the parental or dual-resistant cells (Figure 4). The effect of GDC-0941 on phospho-FOXO1 was difficult to determine, as the level of this protein was very low in cell lysates (Supplementary Figure 3). It is possible that FOXO1 and BCL-2 proteins are regulated through altered protein localization or through other post-translational modifications.

Sensitivity of the dual-resistant K562 cells to the BCL-2 inhibitor, ABT-737, in combination with dasatinib, GDC-0941 or GDC-0973
The BCL-2 family of pro-survival proteins have been implicated in CML disease progression and are regulated by the PI3K pathway in CML cells.²³ BCL-2 was elevated in the dual-resistant K562 cells, however, these cells were insensitive to growth inhibition induced by ABT-737 alone or in combination with dasatinib at clinically relevant exposures ($< 1 \mu\text{M}$; Figure 5). Rather, ABT-737 increased GDC-0941-mediated growth inhibition at clinically relevant exposures (0.1–1 μM) in the dual-resistant but not in the parental cells (Figure 5). These data indicate that, in the dual-resistant cells, PI3K and BCL-2 may cooperate to mediate the resistant phenotype.

A role for FOXO1 in BCR-ABL1 kinase-independent resistance
As protein localization of FOXO1 is regulated by PI3K signaling,^{11,12} we performed immunofluorescence on untreated, dasatinib-treated and GDC-0941-treated parental and dual-resistant K562 cells. FOXO1 expression was very low in the parental cell line with a signal comparable to the IgG

Table 1. Sensitivities of the parental and dual-resistant KCL-22 cells and K562 cells and clones to imatinib, dasatinib, GDC-0941 and GDC-0973

Cell line	Imatinib (GI_{50} , μM)	Dasatinib (GI_{50} , μM)	GDC-0941 (GI_{50} , μM)	GDC-0973 (GI_{50} , μM)
K562 parental	0.3	< 0.001	2	0.88
Dual-resistant cells	> 10	> 10	0.02	1.1
Clone 4	> 10	> 10	0.22	2
Clone 11	> 10	> 10	0.36	8
Clone 12	> 10	> 10	0.29	5
Clone 13	> 10	> 10	0.47	3.5
Clone 17	> 10	> 10	0.1	2.3
Clone 20	> 10	> 10	0.17	0.55
KCL-22 parental	0.28	< 0.001	1.5	1
KCL-22 resistant	> 10	> 10	1.5	3.5

The cells were treated with 0–10 μM of the indicated inhibitors for 72 h, followed by measurement of cell viability by CellTiter-Glo assay. The cell viability after 72 h was corrected relative to time zero (time of treatment). GI_{50} values to all single agents are shown.

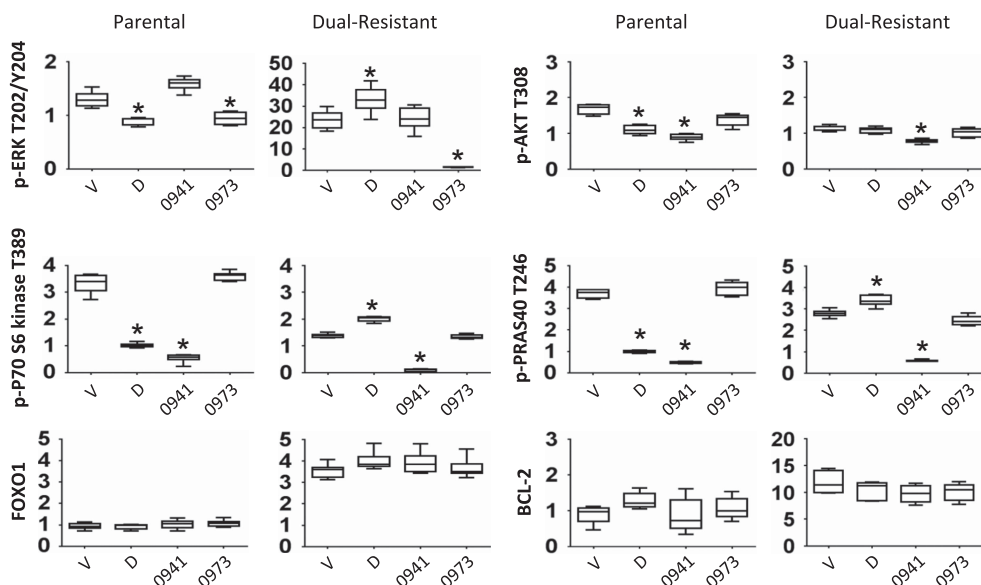


Figure 4. GDC-0941 inhibits phosphorylation of PI3K substrates in the dual-resistant cells. Responsiveness of phospho-c-ABL Y245, phospho-Akt T308, phospho-PRAS40 T246, phospho-p70 S6 kinase T389, FOXO1 and BCL-2 to vehicle (DMSO, V), 100 nM dasatinib (D), 300 nM GDC-0941 (0941) or 300 nM GDC-0973 (0973) treatment for 1 h in parental K562 (Pa) or dual-resistant K562 cells (DR) by reverse-phase protein array. The data were normalized to total protein and log₂-transformed. The error bars represent standard deviation. $*P < 0.05$.

control (not shown). In contrast, FOXO1 expression in the resistant cells was much higher than in the parental cells (Figure 6), in agreement with the RPPA analysis (Figure 2). FOXO1 was sequestered in the cytoplasm in untreated and dasatinib-treated resistant cells. However, after 1 h

treatment with GDC-0941, most FOXO1 protein had translocated into the nucleus (Figure 6). These data suggest that the subcellular localization of FOXO1, and therefore its transcriptional activity, are regulated by PI3K in the dual-resistant cells.

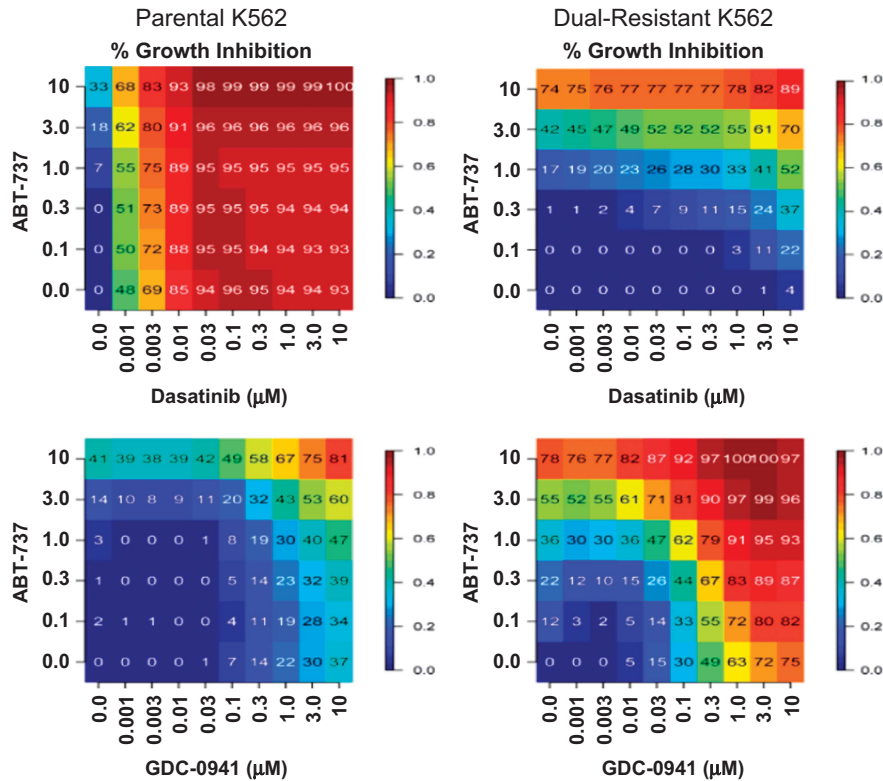


Figure 5. The BCL-2 inhibitor, ABT-737, in combination with GDC-0941, inhibits growth of the dual-resistant but not parental K562 cells. Parental and dual-resistant K562 cells were treated with 0–10 μ M of the BCL-2 inhibitor, ABT-737, alone or in combination with 0–10 μ M dasatinib or GDC-0941. The cell viability after 72 h was measured using a CellTiter-Glo assay and mean percentage growth inhibition derived from quadruplicates at each dose or combination is shown.

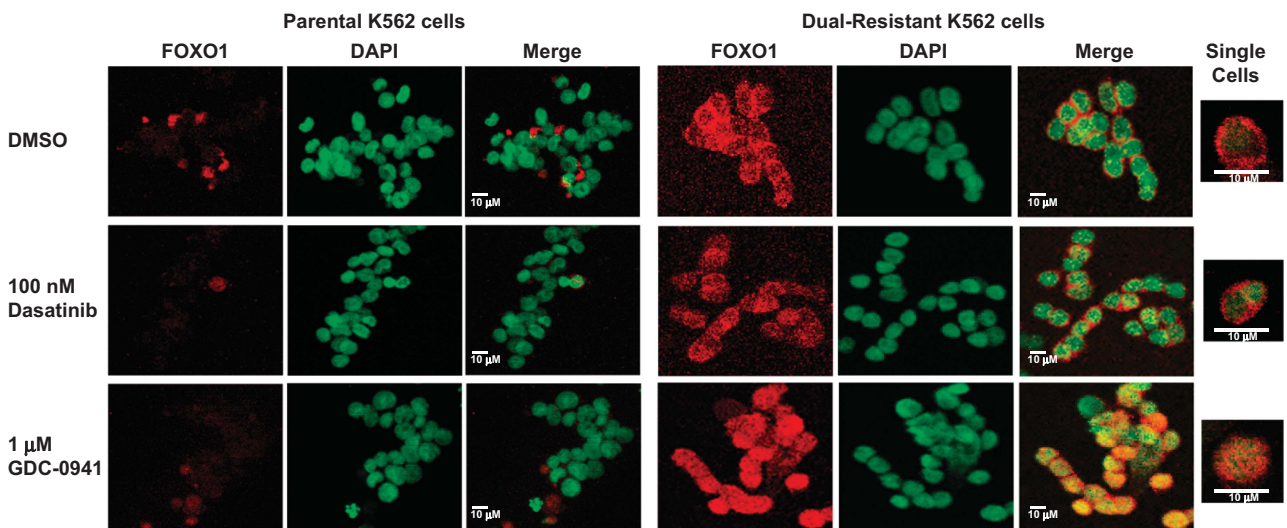


Figure 6. Elevated FOXO1 accumulates in the cytoplasm of the dual-resistant K562 cells and translocates into the nucleus upon GDC-0941 treatment. Immunofluorescence cytochemistry revealed that FOXO1 was localized primarily within the cytoplasm of dual-resistant K562 cells treated with DMSO or 100 nM dasatinib, whereas it was low to undetectable in the parental TKI-sensitive controls. The treatment of dual-resistant K562 cells with 1 μ M GDC-0941 resulted in a translocation of FOXO1 to the nucleus. Representative images of the treatment groups are shown under $\times 40$ magnification using confocal microscopy. For clarity, single-cell images are shown for the dual-resistant cells.

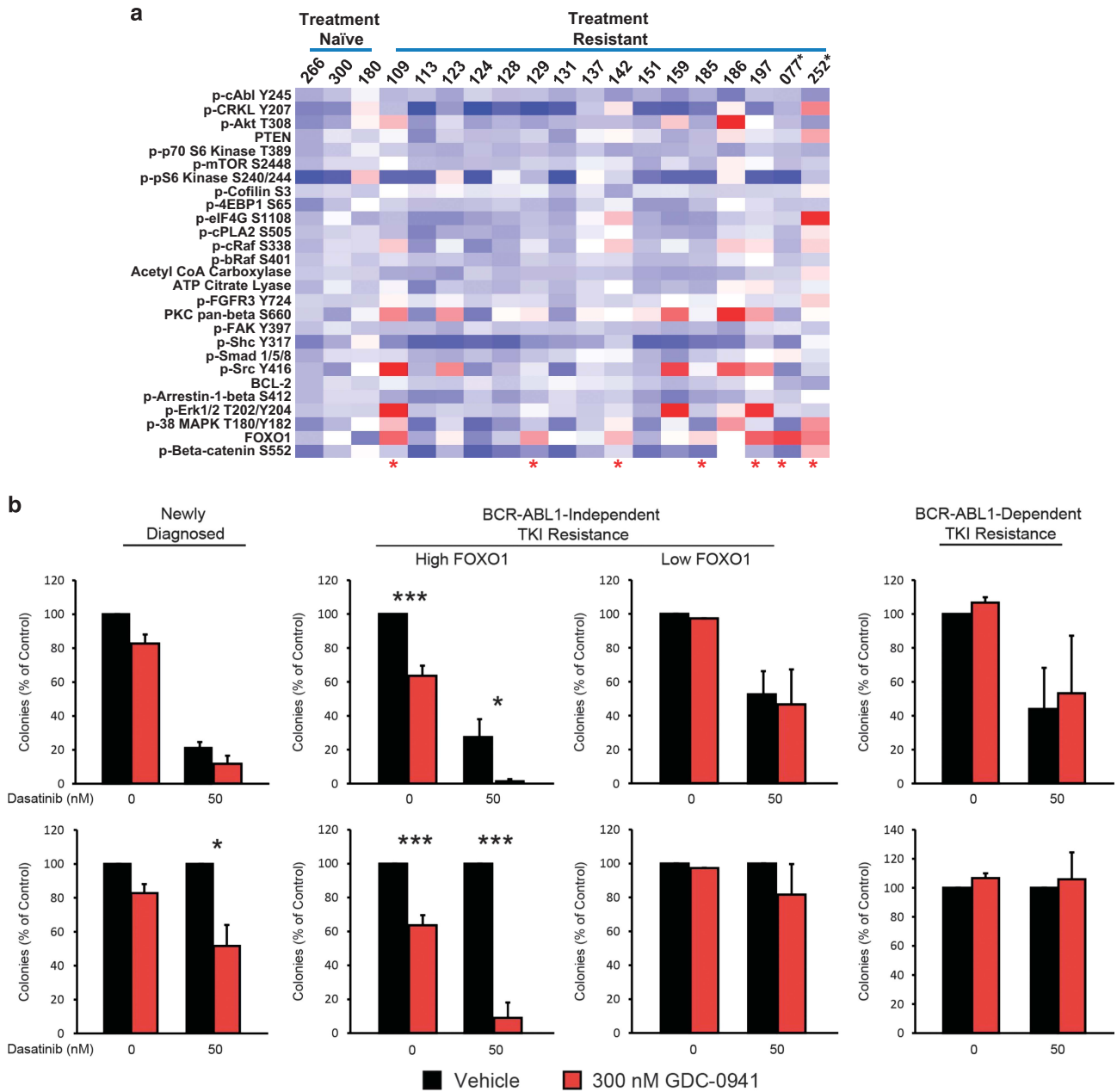


Figure 7. FOXO1 levels are elevated in a subset of relapsed patient samples and are sensitive to GDC-0941-mediated survival inhibition. **(a)** The baseline proteomic signature of TKI-naïve samples (samples 180, 266 and 300) compared with samples from TKI-relapsed patients (resistant) lacking *BCR-ABL1* mutations (samples 109-197) or harboring a *BCR-ABL1* kinase domain mutation (samples 077 and 252). Samples with elevated FOXO1 expression are denoted by a red asterisk. **(b)** TKI-naïve samples (180, 266 and 300) and patient samples with high FOXO1 (077, 109, 142, 185, 197 and 252) or low FOXO1 (123 and 186) were treated with dasatinib (50 nM) and/or GDC-0941 (300 nM) in colony-formation assays. The data represents percent of vehicle-treated controls. The error bars represent standard deviation. * $P < 0.05$, *** $P < 0.001$.

To further clarify the role of FOXO1 in ABL-TKI resistance, we assessed the effect of FOXO1 knockdown on the response of parental and dual-resistant K562 cells to dasatinib and GDC-0941. A non-targeting sequence and shRNAs targeting GAPDH and FOXO3a were used as controls (Supplementary Table S3). In parental K562 cells, neither FOXO1 nor FOXO3a knockdown had any effect on the response to either drug. In the dual-resistant K562 cells, FOXO1 but not FOXO3a knockdown significantly sensitized the cells to dasatinib while modestly attenuating the sensitivity of these cells to GDC-0941 (Supplementary Figure S4).

Sensitivity of CD34⁺-enriched progenitor cells from newly diagnosed, treatment-naïve patients and ABL-TKI-relapsed patients to dasatinib and GDC-0941

To determine whether any relapsed patient samples had elevated FOXO1 expression, and to see if these samples were sensitive to GDC-0941, we established a panel of samples from patients who had relapsed from two or more prior ABL-TKI therapies in a *BCR-ABL1* kinase-independent manner (Supplementary Table S1). These samples harbored no explanatory *BCR-ABL1* kinase domain mutations or amplifications, and demonstrated reduced

phospho-CRKL upon treatment with dasatinib (Supplementary Figure 2b). For comparison, we included three samples from treatment-naïve patients and two samples from patients with known *BCR-ABL1* kinase domain mutations. First, we identified which proteins were differentially expressed or phosphorylated in these samples using RPPA. Second, we characterized the sensitivity of some of the patient samples to GDC-0941 alone or with dasatinib using colony-formation assays. Baseline RPPA expression data from the relapsed patients was normalized to data from the three ABL-TKI treatment-naïve patients, confirming that a subset of the relapsed patients had elevated FOXO1 levels in the absence of *BCR-ABL1* kinase domain mutations (patient samples 109, 129, 142, 185 and 197; Figure 7a; Supplementary Table S1) but not FOXO3a or FOXO4 (data not shown). Unexpectedly, normalized RPPA data from two relapsed patient-derived specimens harboring the *BCR-ABL1* kinase domain mutations, E255K (patient 252) or T315I (patient 077), also demonstrated elevated FOXO1 levels.

To assess the effects of GDC-0941 on survival of primary cells *ex vivo*, we performed colony-formation assays in the presence of dasatinib (50 nM) and/or GDC-0941 (300 nM). Figure 7b shows colony formation data as percent of surviving colonies normalized to the vehicle control (top), or normalized to both vehicle- and dasatinib-treated controls (bottom). In samples from newly diagnosed CML patients (patients 180, 266 and 300), GDC-0941 alone had no significant effect on colony formation; however, GDC-0941 did significantly reduce colony formation in the presence of dasatinib when normalized to the dasatinib alone group (Figure 7b, left). In four patient samples with *BCR-ABL1* kinase-independent resistance and elevated levels of FOXO1 (patients 109, 142, 185 and 197), GDC-0941 significantly reduced survival alone, but even more so in the presence of dasatinib (Figure 7b, middle). In contrast, GDC-0941 had no effect on samples with *BCR-ABL1* kinase-independent resistance and low levels of FOXO1 (patients 123 and 186; Figure 7b, middle), or in samples from patients with *BCR-ABL1* kinase domain mutations, despite having elevated levels of FOXO1 (patients 077 and 252; Figure 7b, right). Surprisingly, dasatinib alone significantly reduced colony formation in all ABL-TKI-resistant samples (Figure 7), likely due to inhibition of the KIT pathway, which may be activated by the CC100 cytokine cocktail required for these assays. Alternatively, it may reflect microenvironment-mediated resistance mechanisms that are present in the body of the patient but not in colony-formation assays. Thus, in a subset of patients who relapse after sequential ABL-TKI therapy without *BCR-ABL1* kinase domain mutations, FOXO1 levels are elevated, rendering the cells sensitive to combined treatment with dasatinib and the PI3K inhibitor, GDC-0941.

DISCUSSION

Acquired resistance is a major challenge for long-term effective use of targeted cancer therapies. Treatment of patients with ABL-TKI therapy has transformed CML from a fatal to a chronic disease, but many patients who remain on these drugs for a prolonged time develop acquired drug resistance. Although kinase domain mutations are the best characterized mechanism of acquired resistance, they fail to explain many cases of clinical ABL-TKI failure. In the present study, we use sequencing and proteomics-based approaches to identify FOXO1 as a mediator of *BCR-ABL1* kinase-independent resistance in dual-resistant K562 cells, but not in KCL-22 cells harboring the T315I mutation.

RPPA data revealed that the MAPK and PI3K pathways were differentially expressed between the parental and dual-resistant K562 cells (Figure 2) and activated by dasatinib only in the dual-resistant cells. However, only PI3K inhibition impaired the growth and survival of these cells (Figure 3). This data contrasts with a recent report showing that the

MEK inhibitor, trametinib, in combination with imatinib can effectively kill imatinib-resistant CML cells, and that PI3K signaling is not involved in this resistance.²⁴ There are likely to be multiple *BCR-ABL1* kinase-independent mechanisms of resistance in CML cells.^{7–10}

Cytoplasmic retention of FOXO1 has been reported in paclitaxel-resistant ovarian cancer cell lines and patient samples.²⁵ Importantly, FOXO1 was retained at elevated levels in the cytoplasm of dual-resistant but not parental K562 cells (Figure 6). Chronic exposure of K562 cells to doxorubicin can lead to activation of FOXO3a, which upregulates the expression of drug-resistance genes.²⁶ However, in our hands, knockdown of FOXO3a had no effect on the growth of dual-resistant K562 cells, either alone or when cultured in dasatinib or GDC-0941 (Supplementary Figure S4). Only knockdown of FOXO1 restored the effect of dasatinib on dual-resistant K562 cells, while at the same time abrogating the effects of GDC-0941 (Supplementary Figure S4). Thus, stable knockdown experiments confirmed the involvement of FOXO1 in the dual-resistant K562 cells, in addition to being a marker of PI3K inhibitor sensitivity in certain kinase-independent ABL-TKI-resistant cells.

In CP-CML CD34⁺ cells from newly diagnosed patients, FOXO transcription factors were shown to be regulated by *BCR-ABL1* kinase activity.¹⁷ Alternatively, the activation of FOXO family members has been shown to activate proapoptotic genes and apoptosis in hematopoietic cells.²⁷ In contrast to newly diagnosed CML patient samples,¹⁷ the expression and localization of FOXO1 in cells with dual resistance appears to be independent of *BCR-ABL1* kinase activity.

Despite the elevated levels of BCL-2 in the resistant cell lines and the synergy between GDC-0941 and ABT-737, none of the patient samples evaluated had elevated BCL-2. It is possible that high BCL-2 in the dual-resistant cells was an artifact of *in vitro* culturing or not enough patient samples were screened to detect it.

We conclude that cytoplasmic FOXO1 is elevated in the dual-resistant K562 cells and in a subset of samples from relapsed patients. The cell lines and patient samples that had high FOXO1 with a *BCR-ABL1*-independent mechanism of resistance were sensitive to PI3K inhibition alone or in combination with dasatinib. Therefore, treatment with a regimen containing PI3K inhibitors like GDC-0941 may enhance the response of patients that have undergone sequential ABL-TKI therapy and relapsed with *BCR-ABL1* kinase-independent mechanisms of resistance involving elevated cytoplasmic FOXO1 levels.

CONFLICT OF INTEREST

Some of the authors are employees of Roche/Genentech. We used our in-house molecules, GDC-0941 and GDC-0973, as representative PI3K and MEK kinase inhibitors, respectively. These molecules have been published and are available from commercial sources. Furthermore, our findings should be applicable to similar inhibitors from other sources. The remaining authors declare no conflict of interest.

ACKNOWLEDGEMENTS

This work was supported in part by the National Cancer Institute (NCI) R01CA178397 (to MWD and TO). AME was supported by NCI T32CA093247, a Career Development Award from the Leukemia and Lymphoma Society (5090–12), and currently funded through a Scholar Award from the American Society of Hematology. AME acknowledges support from the National Institutes of Health Loan Repayment Program.

REFERENCES

- 1 O'Hare T, Zabriskie MS, Eiring AM, Deininger MW. Pushing the limits of targeted therapy in chronic myeloid leukaemia. *Nat Rev Cancer* 2012; **12**: 513–526.

- 2 Kantarjian HM, Larson RA, Guilhot F, O'Brien SG, Mone M, Rudoltz M *et al*. Efficacy of imatinib dose escalation in patients with chronic myeloid leukemia in chronic phase. *Cancer* 2009; **115**: 551–560.
- 3 Hochhaus A, Kreil S, Corbin AS, La Rosee P, Muller MC, Lahaye T *et al*. Molecular and chromosomal mechanisms of resistance to imatinib (STI571) therapy. *Leukemia* 2002; **16**: 2190–2196.
- 4 Soverini S, Colarossi S, Gnani A, Rosti G, Castagnetti F, Poerio A *et al*. Contribution of ABL kinase domain mutations to imatinib resistance in different subsets of Philadelphia positive patients: by the GIMEMA Working Party on Chronic Myeloid Leukemia. *Clin Cancer Res* 2006; **12**: 7374–7379.
- 5 Soverini S, Eide CA, Tantravahi SK, Vellore NA, Estrada J, Nicolini FE *et al*. BCR-ABL1 compound mutations combining key kinase domain positions confer clinical resistance to ponatinib in Ph chromosome-positive leukemia. *Cancer Cell* 2014; **26**: 428–442.
- 6 Nambu T, Araki N, Nakagawa A, Kuniyasu A, Kawaguchi T, Hamada A *et al*. Contribution of BCR-ABL-independent activation of ERK1/2 to acquired imatinib resistance in K562 chronic myeloid leukemia cells. *Cancer Sci* 2010; **101**: 137–142.
- 7 Quentmeier H, Eberth S, Romani J, Zaborski M, Drexler HG. BCR-ABL1-independent PI3Kinase activation causing imatinib-resistance. *J Hematol Oncology* 2011; **4**: 6.
- 8 Eiring AM, Page BD, Kraft IL, Mason CC, Vellore NA, Resettec D *et al*. Combined STAT3 and BCR-ABL1 inhibition induces synthetic lethality in therapy-resistant chronic myeloid leukemia. *Leukemia* 2015; **29**: 586–597.
- 9 Traer E, MacKenzie R, Snead J, Agarwal A, Eiring AM, O'Hare T *et al*. Blockade of JAK2-mediated extrinsic survival signals restores sensitivity of CML cells to ABL inhibitors. *Leukemia* 2012; **26**: 1140–1143.
- 10 Burchert A, Wang Y, Cai D, von Bubnoff N, Paschka P, Muller-Brusselbach S *et al*. Compensatory PI3-kinase/Akt/mTor activation regulates imatinib resistance development. *Leukemia* 2005; **19**: 1774–1782.
- 11 Tzivion G, Dobson M, Ramakrishnan G. FoxO transcription factors; Regulation by AKT and 14-3-3 proteins. *Biochim Biophys Acta* 2011; **1813**: 1938–1945.
- 12 Tzivion G, Hay N. PI3K-AKT-FoxO axis in cancer and aging. *Biochim Biophys Acta* 2011; **1813**: 1925.
- 13 Arden KC. Multiple roles of FOXO transcription factors in mammalian cells point to multiple roles in cancer. *Exp Gerontol* 2006; **41**: 709–717.
- 14 Chen J, Gomes AR, Monteiro LJ, Wong SY, Wu LH, Ng TT *et al*. Constitutively nuclear FOXO3a localization predicts poor survival and promotes Akt phosphorylation in breast cancer. *PLoS One* 2010; **5**: e12293.
- 15 Kharas MG, Okabe R, Ganis JJ, Gozo M, Khandan T, Paktinat M *et al*. Constitutively active AKT depletes hematopoietic stem cells and induces leukemia in mice. *Blood* 2010; **115**: 1406–1415.
- 16 Naka K, Hoshii T, Muraguchi T, Tadokoro Y, Ooshio T, Kondo Y *et al*. TGF-beta-FOXO signalling maintains leukaemia-initiating cells in chronic myeloid leukaemia. *Nature* 2010; **463**: 676–680.
- 17 Pellicano F, Scott MT, Helgason GV, Hopcroft LE, Allan EK, Aspinall-O'Dea M *et al*. The antiproliferative activity of kinase inhibitors in chronic myeloid leukemia cells is mediated by FOXO transcription factors. *Stem Cells* 2014; **32**: 2324–2337.
- 18 Yuan H, Wang Z, Gao C, Chen W, Huang Q, Yee JK *et al*. BCR-ABL gene expression is required for its mutations in a novel KCL-22 cell culture model for acquired resistance of chronic myelogenous leukemia. *J Biol Chem* 2010; **285**: 5085–5096.
- 19 O'Hare T, Shakespeare WC, Zhu X, Eide CA, Rivera VM, Wang F *et al*. AP24534, a pan-BCR-ABL inhibitor for chronic myeloid leukemia, potently inhibits the T315I mutant and overcomes mutation-based resistance. *Cancer Cell* 2009; **16**: 401–412.
- 20 Bourgon R, Lu S, Yan Y, Lackner MR, Wang W, Weigman V *et al*. High-throughput detection of clinically relevant mutations in archived tumor samples by multiplexed PCR and next-generation sequencing. *Clin Cancer Res* 2014; **20**: 2080–2091.
- 21 Medina PP, Romero OA, Kohno T, Montuenga LM, Pio R, Yokota J *et al*. Frequent BRG1/SMARCA4-inactivating mutations in human lung cancer cell lines. *Hum Mutat* 2008; **29**: 617–622.
- 22 Merel P, Hoang-Xuan K, Sanson M, Moreau-Aubry A, Bijlsma EK, Lazaro C *et al*. Predominant occurrence of somatic mutations of the NF2 gene in meningiomas and schwannomas. *Genes Chromosomes Cancer* 1995; **13**: 211–216.
- 23 Tzifi F, Economopoulou C, Gourgiotis D, Ardavanis A, Papageorgiou S, Scorilas A. The role of BCL2 family of apoptosis regulator proteins in acute and chronic leukemias. *Adv Hematol* 2012; **2012**: 524308.
- 24 Ma L, Shan Y, Bai R, Xue L, Eide CA, Ou J *et al*. A therapeutically targetable mechanism of BCR-ABL-independent imatinib resistance in chronic myeloid leukemia. *Sci Transl Med* 2014; **6**: 252ra121.
- 25 Goto T, Takano M, Hirata J, Tsuda H. The involvement of FOXO1 in cytotoxic stress and drug-resistance induced by paclitaxel in ovarian cancers. *Br J Cancer* 2008; **98**: 1068–1075.
- 26 Hui RC, Gomes AR, Constantinidou D, Costa JR, Karadedou CT, Fernandez de Mattos S *et al*. The forkhead transcription factor FOXO3a increases phosphoinositide-3 kinase/Akt activity in drug-resistant leukemic cells through induction of PIK3CA expression. *Mol Cell Biol* 2008; **28**: 5886–5898.
- 27 Burgering BM, Medema RH. Decisions on life and death: FOXO Forkhead transcription factors are in command when PKB/Akt is off duty. *J Leuk Biol* 2003; **73**: 689–701.



This work is licensed under a Creative Commons Attribution-NonCommercial-NoDerivs 4.0 International License. The images or other third party material in this article are included in the article's Creative Commons license, unless indicated otherwise in the credit line; if the material is not included under the Creative Commons license, users will need to obtain permission from the license holder to reproduce the material. To view a copy of this license, visit <http://creativecommons.org/licenses/by-nc-nd/4.0/>

Supplementary Information accompanies this paper on the Leukemia website (<http://www.nature.com/leu>)